

## A METHOD FOR REDUCING MASS INCONSISTENCY IN CMAQ AND ITS IMPACTS ON CHEMICAL SPECIES CONCENTRATION

Fuquan Yang\*, Jack Chen

Institute for Chemical Process and Environment Technology, National Research Council of Canada, Ottawa, Ontario, Canada

### 1. INTRODUCTION

Mass inconsistency in the advection process of an air quality model is the result of imbalances between the air mass flux inflow and outflow by winds and air density. Currently two mass adjustment methods, "DENRATE" and "YAMO", are implemented in the Community Multi-scale Air Quality (CMAQ) model to remedy the effects of mass inconsistency on chemical species concentrations (CMAQ v4.6 Operational Guidance Document).

The first approach, "DENRATE", retains the horizontal contravariant winds from the Meteorology-Chemistry Interface Processor (MCIP) (Byun, 1999). The chemical species concentrations are renormalized by the ratio of the CMAQ advected air density to the density from the Meteorology-Chemistry Interface Processor (MCIP) after each advection time step.

The second approach is the "YAMO" method (Odman et al., 2000), available since CMAQ version 4.5. This approach also retains the horizontal contravariant winds from MCIP. However, it recalculates the contravariant vertical velocity before the advection process under constraints of satisfying the mass continuity equation. There is no change to the air density field from the input meteorological model. The common characteristic of these two approaches is that they keep both of the horizontal wind components from the input meteorological model.

The objective of this paper is to test an algorithm that reduces the mass inconsistency adjustments in CMAQ by adjusting the input horizontal winds. This algorithm keeps air density from the MCIP unchanged. It was implemented in MCIP and was used together with the "DENRATE" method. Its impacts on chemical species concentration were also investigated.

\*Corresponding author: Dr. Fuquan Yang, Institute for Chemical Process and Environment Technology, National Research Council of Canada, Ottawa, Canada, E-mail: Fuquan.Yang@nrc-cnrc.gc.ca

### 2. A FILTER FOR REDUCING MASS INCONSISTENCY

#### 2.1 Mass inconsistency in CMAQ

To quantify the mass inconsistency in the current CMAQ advection scheme, a simple tracer simulation was carried out for a 25-hour period (UTC 00:00 1 July to 00:00 2 July, 2002.). The model system included the non-hydrostatic MM5 version 3.7 (Dudhia et al., 2006), MCIP version 3.3 and CMAQ version 4.6.

The CMAQ domain had a horizontal grid resolution of 36-km and 15 vertical layers. Chemistry, deposition and diffusion processes in CMAQ were turned off to isolate the effects of advection on tracer concentrations. The initial and boundary conditions of the passive tracer were set to be 1 ppm. Ideally, the tracer concentration of a grid box that meets mass consistency requirement remains to be 1 ppm. The larger the deviation of the tracer concentration from 1 ppm in a grid box, the more serious the mass inconsistency is.

Fig. 1 shows the tracer concentration after 10 hours simulation with the default mass adjustment method in CMAQ. For most areas east of the Rocky Mountains, where the terrain is low and flat, the tracer concentrations were close to 1 ppm (0.95 - 1.05ppm). If all the factors that possibly lead to the mass inconsistency are taken into account (Byun, 1999), the wind and air density from MCIP have the property of meeting the mass consistency requirement to a high degree in these regions.

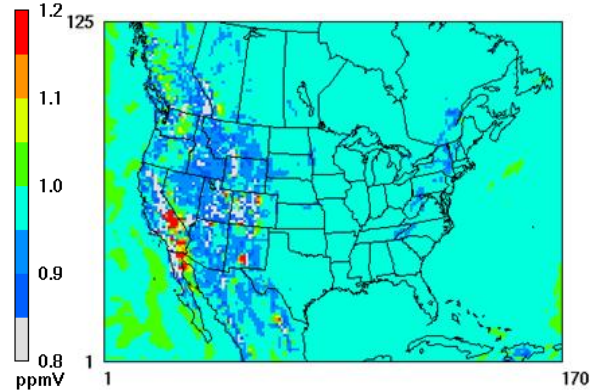


Fig. 1. Tracer concentration at 1000 UTC, 1 July 2002.

The mass inconsistency problem becomes pronounced in high and steep terrain regions west of the Rocky Mountains, such as in California. Fig. 2 illustrates the hourly tracer concentrations in two nearby grid boxes, (23, 56) and (25, 54), for a tracer run in which the mass adjustment was turned off. Both grid boxes are geographically located in California. The mass budget variations of the two grids were nearly opposite in terms of their deviations from 1 ppm from hour 5 to hour 20. This indicates that the air mass deficit in grid box (23, 56) can be partly attributed to the mass excess in grid box (25, 54). The large mass-budget gradient between these nearby grid boxes implies the existence of high frequency short waves in the western part of the domain.

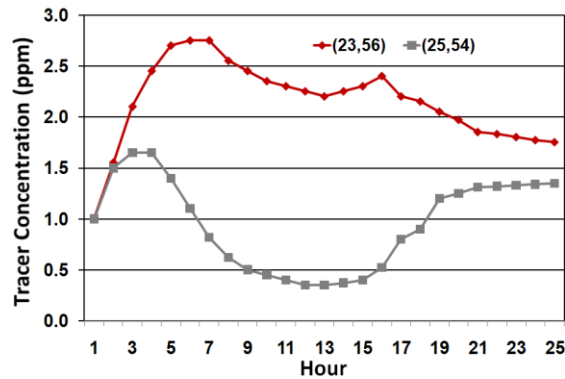


Fig. 2. Diurnal variations of tracer concentration in two nearby grid boxes, (23, 56) and (25, 54).

## 2.2 A low-pass smoother-desmoother filter

Considering the existence of the high frequency short waves in the western part of the domain, we can reduce the large mass-budget gradient by applying a filter that can suppress the high frequency short waves while retaining large scale features. In this study, we selected the five-point smoother-desmoother filter (Guo et al., 1994) because it can remove waves with wavelength  $2\Delta x$  ( $\Delta x$  is the model grid size), but leave long waves almost unaffected. This is a low-pass filter that passes the low-frequency components of the waves but attenuates the higher frequency components. This filter is utilized in the TERRAIN program of the MM5 model to smooth out the high frequency components in terrain height fields. The mathematical formula of the filter is:

$$\hat{X}(I, J) = X(I, J) + \alpha * [0.5 * (X(I+1, J) + X(I-1, J)) - X(I, J)] \quad (1)$$

$$X^*(I, J) = \hat{X}(I, J) + \alpha * [0.5 * (\hat{X}(I, J+1) + \hat{X}(I, J-1)) - \hat{X}(I, J)] \quad (2)$$

where  $X$  is the variable to be smoothed,  $X^*$  is the smoothed variable and  $\alpha$  is the smoothing factor.

There are two steps involved in a single pass in this procedure. First, the two equations are applied with  $\alpha = 0.5$  to smooth out short waves, and the filter is then applied again to the intermediate results with  $\alpha = -0.52$  to recover waves with wavelength larger than  $2\Delta x$ .

Fig. 3 shows the response of the filter for one, two and three passes respectively. More short waves are smoothed out when the filter is applied more than one time. For example, less than 15% of the waves with  $4\Delta x$  wavelength are smoothed after one pass. However, more than 90% of these waves are smoothed out after three passes. In the following study, the filter was applied one time to the MCIP horizontal contravariant wind fields only.

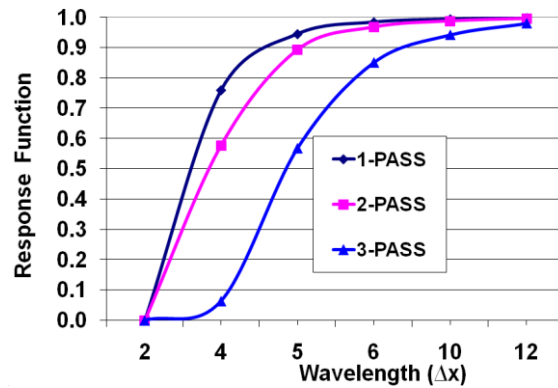


Fig. 3. Response functions after one, two and three passes of the smoother-desmoother filter, respectively.

## 2.3 Effect on horizontal wind fields

The filter was applied to the two components of the contravariant horizontal wind in the MCIP for the month of July 2002. Fig. 4(a) and Fig. 4(b) show the west-east component of the horizontal contravariant wind (UWIND) before and after the filter was applied. Fig 4(c) shows the difference between them.

The resemblance of Fig. 4(a) and Fig. 4(b) indicates that the filter did not change the large-scale pattern of the horizontal wind fields. However, large wind differences between -4.8m/s and 4.7m/s were found at high and steep terrain areas west of the Rocky Mountains in the western part of the domain. The differences were minimal in the maritime and other low flat areas. This implied that only the high frequency short waves were smoothed out.

The situation was similar for the south-north component of the horizontal contravariant wind (VWIND, figure not shown). The high frequency

waves were filtered out while the large scale components were retained.

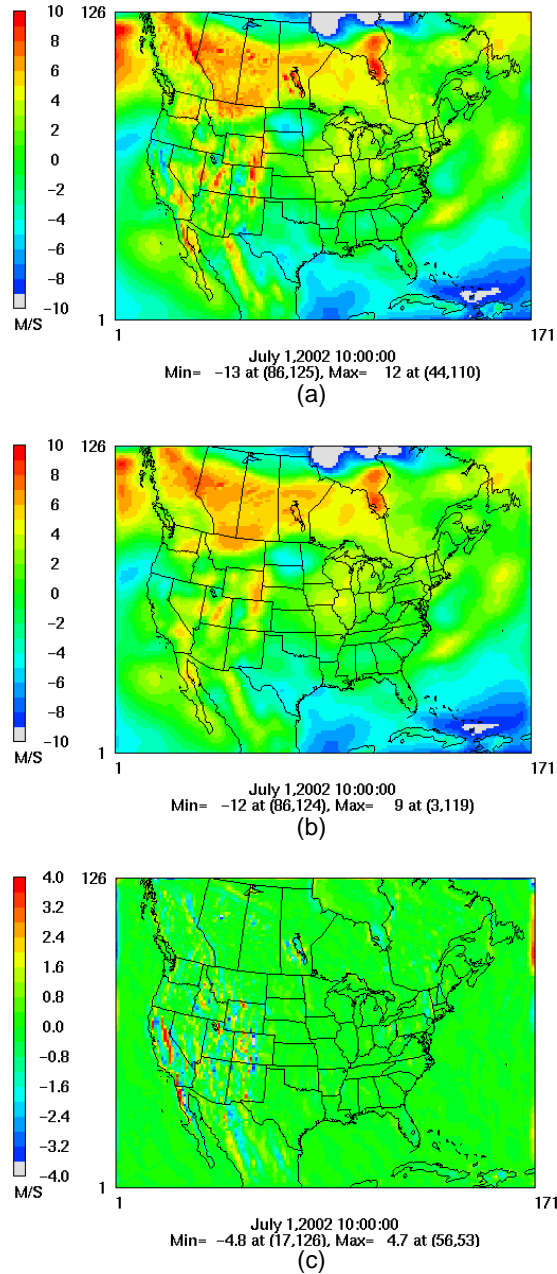


Fig. 4. East-west component of contravariant horizontal wind at 10 UTC, July 1, 2002; (a) before the filter was applied, (b) after the filter was applied, and (c) difference between (b) and (a).

Table 1 summarizes the performance statistics of the horizontal wind speed and direction across the domain for the whole month, before and after the filter was applied. Overall, the mean wind speed was reduced slightly by 0.04

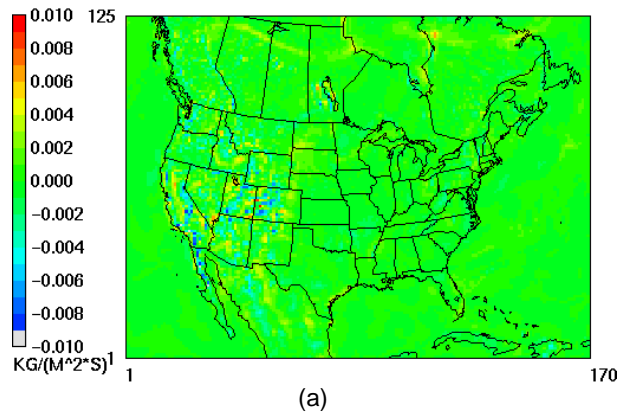
m/s and the standard deviation was reduced from 2.4 to 1.6. However, since the large-scale patterns were not altered, the mean bias and mean error did not change significantly. The overall correlation coefficient (R) varied by less than 1%. From the perspective of domain wide statistics, the filter had little impact on the horizontal wind speed and wind direction.

Table 1. Performance statistics for wind speed (m/s) and wind direction (degree) before and after the filter was applied.

| Statistics            | Wind speed |        | Wind direction |        |
|-----------------------|------------|--------|----------------|--------|
|                       | Before     | After  | Before         | After  |
| Mean                  | 3.35       | 3.31   | 207            | 206    |
| Deviation             | 2.35       | 1.60   | 89.76          | 89.56  |
| Mean Bias             | -0.58      | -0.62  | -11.65         | -11.27 |
| Normalized Mean Bias  | -14.7%     | -15.8% | -5.62%         | -5.46% |
| Mean Error            | 1.6        | 1.6    | 67.1           | 66.9   |
| Normalized Mean Error | 40.7%      | 40.6%  | 32.4%          | 32.4%  |
| R                     | 0.53       | 0.52   | 0.35           | 0.34   |

## 2.4 Effect on vertical wind

Since the contravariant vertical velocity is a derived variable based on the contravariant horizontal wind and Jacobian in MCIP, it may be altered due to the changes of contravariant horizontal winds. The change of the Jacobian and air density weighted contravariant vertical velocity (WHAT\_JD) in MCIP can be used as a surrogate for the changes of contravariant vertical velocity because air density and Jacobian were unaltered by the filter. Fig. 5 (a) and Fig. 5(b) show the WHAT\_JD before and after the filter was applied and Fig. 5(c) shows the difference between them.



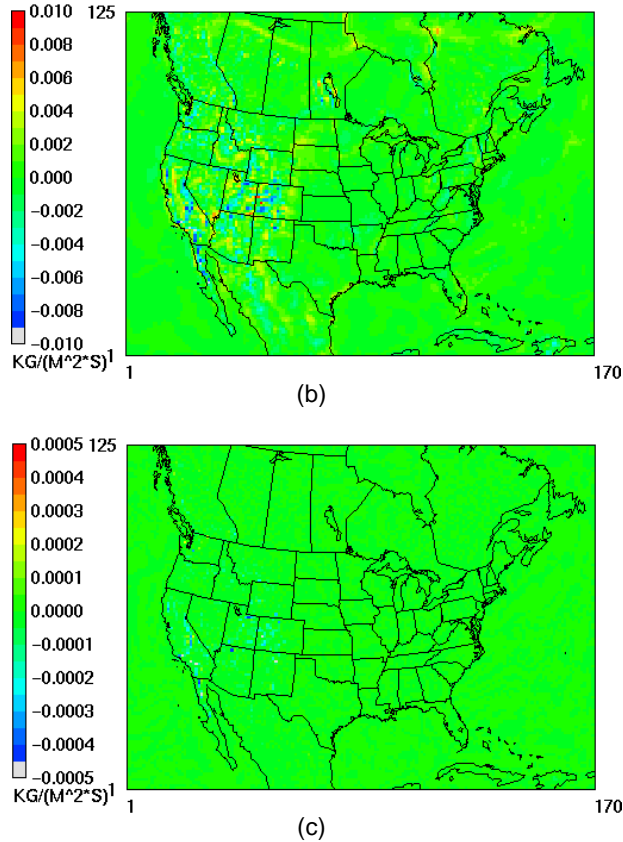


Fig. 5. Jacobian and air density weighted contravariant vertical velocity at 10 UTC, July 1, 2002; (a) before the filter was applied, (b) after the filter was applied, (c) difference between (b) and (a).

The filter had little effect on the contravariant vertical velocity. The largest change was found west of the Rocky Mountains, with +0.0002 kg/(m<sup>2</sup>\*s) at grid (21, 90), and -0.0007 kg/(m<sup>2</sup>\*s) at grid (21, 49). This indicates that the filter caused a less than 2% change in the contravariant vertical velocity and most of the changes occurred at grid cells where the mass inconsistencies were serious.

### 3. IMPACTS ON MASS ADJUSTMENT IN CMAQ

The “DENRATE” approach in CMAQ corrects chemical species concentration based on the ratio of advected air density in CMAQ to the interpolated air density from MCIP at each advection step (Byun et al., 1999). Here the ratio is called the mass adjustment ratio. Fig. 6(a) shows the domain maximum and domain minimum mass adjustment ratio from the tracer simulation. The domain maximum mass adjustment ratio was reduced by approximately

10% at each hour and the domain minimum mass adjustment had little change. Fig. 6(b) shows that the standard deviation across the domain was also decreased by about 20%-30%. This implies an improved mass consistency between the wind fields and air density from MCIP after the filter was applied.

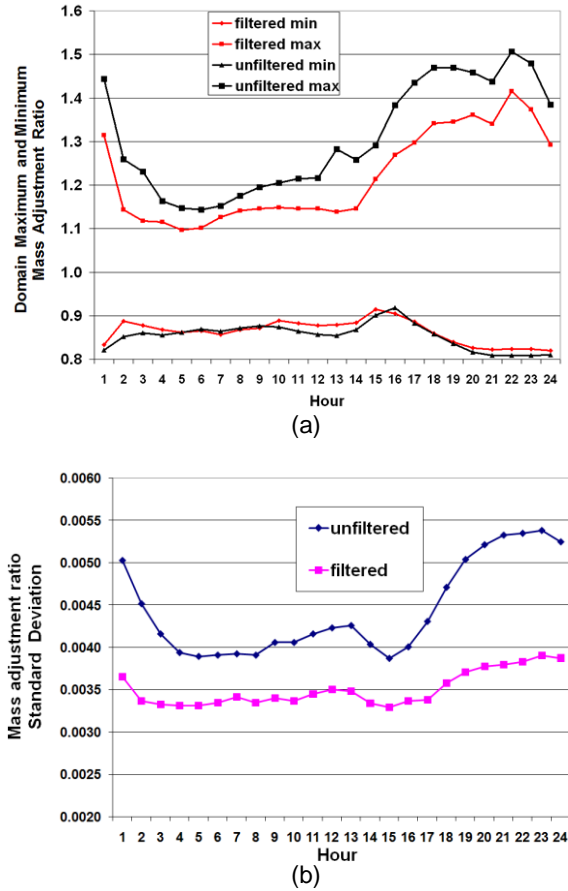


Fig 6. Comparison of the hourly mass adjustment ratio of the simulation, (a) domain maximum and domain minimum, (b) standard deviation across the domain

### 4. IMPACTS ON CHEMICAL SPECIES CONCENTRATION IN CMAQ

To evaluate the impacts on chemical species concentrations, two CMAQ simulations were carried out for the month of July, 2002 with the unfiltered and filtered horizontal wind, respectively. The full model chemistry (saprc99\_ae4\_aq) and physics were used in the simulations. Results from the first two days of each simulation were discarded for spin-up. The domain ozone performance statistics were calculated for both of the two runs.

Table 2 summarizes the hourly ozone model performance statistics averaged over 1245 ozone observation sites in the US and Canada. Overall, just like the comparisons for wind speed and wind direction, the domain-wide statistics remained similar. This result is reasonable because the performance statistics reflect the properties of large-scale ozone patterns across the whole domain for the whole period. The small-scale and short-period high frequency oscillations in ozone concentrations were averaged and smoothed out over space and time.

Table2. Performance statistics for ozone before and after the filter is applied

| Statistics            | Ozone         |              |
|-----------------------|---------------|--------------|
|                       | Before filter | After filter |
| Mean Bias (ppb)       | 9.3           | 9.3          |
| Normalized Mean Bias  | 26%           | 26%          |
| Mean Error (ppb)      | 14.4          | 14.4         |
| Normalized Mean Error | 40%           | 40%          |
| R                     | 0.71          | 0.71         |

Fig.7 shows the difference of averaged daily maximum ozone concentration across the simulation period. The largest difference was found in California where the changes in horizontal wind fields were also large (see Fig. 4). The maximum change of +2.17 ppbv occurred at grid (25, 44) and the minimum change of -2.41 ppbv occurred at grid (24, 46). These differences can be attributed to high emissions and the larger filter influences on the horizontal winds.

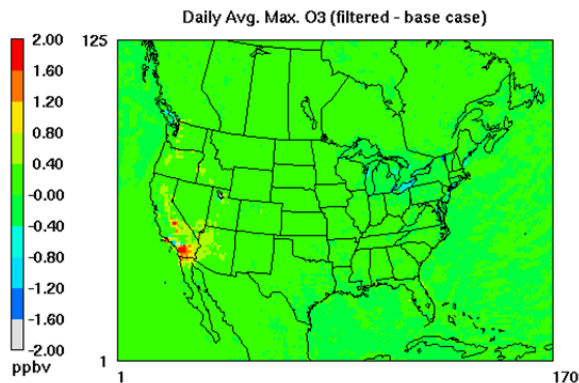


Fig. 7. Difference of the average daily maximum ozone concentration before and after the filter was applied

#### 4.2. Comparisons of ozone in California

Fig. 9 shows examples of ozone concentration differences caused by the filter from six selected ozone monitoring sites in California (Fig. 8) where measured ozone concentrations were high. The CMAQ modeled ozone concentrations from the two simulations were compared with the measured hourly ozone concentrations for the period from July 5 to July 14, 2002. The lower portion of each figure shows the hourly ozone difference between the two simulations.

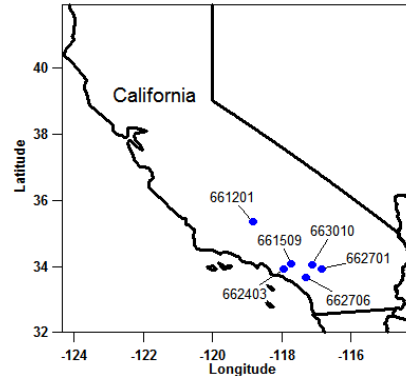
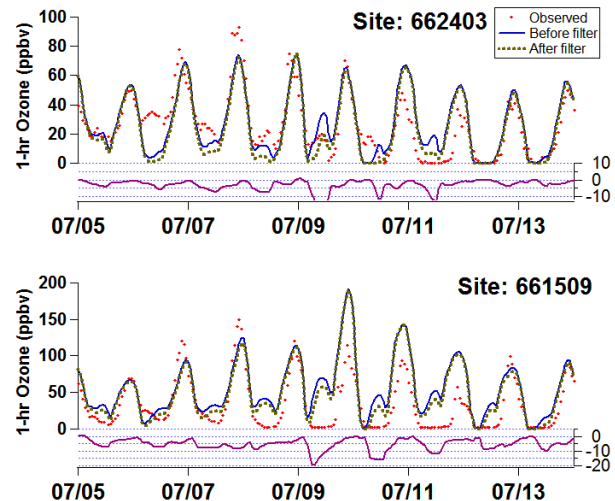


Fig. 8. Locations of the selected ozone monitoring sites

In general, CMAQ captured the overall ozone concentrations well at most of the sites. The magnitudes of the daily maximum were captured better than that of the daily minimum in the model. Although CMAQ sometimes missed the daily maximum ozone at some sites, it consistently over predicted the night time ozone at all sites.



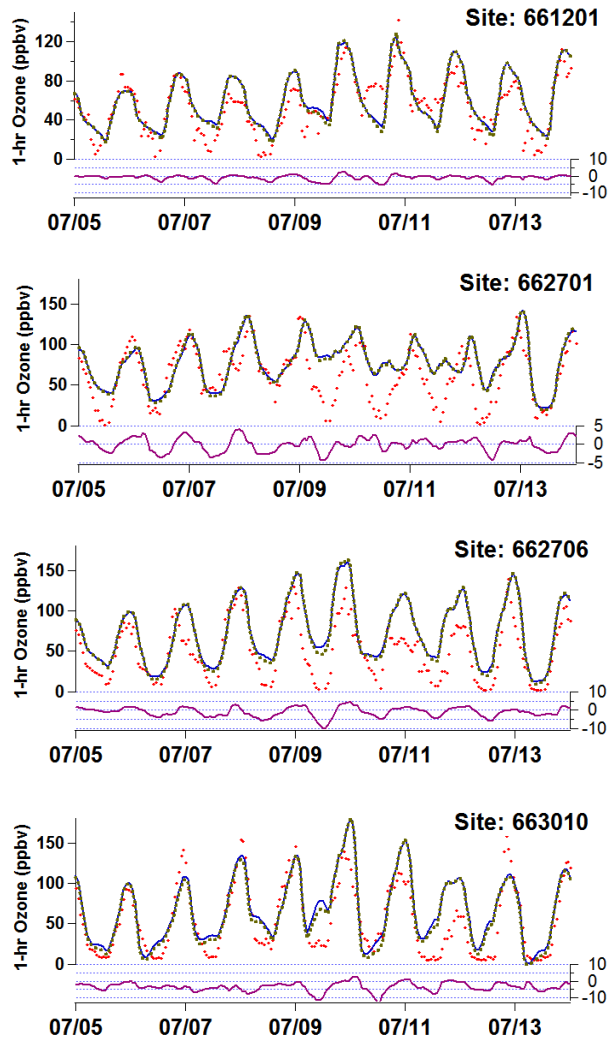


Fig. 9. Comparison of ozone hourly concentration at selected measurement sites in California before and after the filter is applied. The lower part of each figure shows the ozone difference of the two runs.

After the filter was applied, there was little change to the overall ozone trends. However, fine scale changes were observed, especially in the nighttime during high ozone conditions. For example, at the measurement site east of Los Angeles (Site 661509), the nighttime ozone level was reduced by 20 ppb (-37%). This implies that the filter has the potential of alleviating the problem of overpredicting nighttime ozone in CMAQ.

The effects of the filter on daytime ozone were not as pronounced as on nighttime ozone. A possible reason is that the filter had larger effect on nighttime wind fields than that of daytime wind fields. Further investigations are needed.

## 5. CONCLUSION

A numerical smoother-desmoothing filter was applied to the horizontal contravariant wind from non-hydrostatic MM5/MCIP before the wind was used in the CMAQ advection processes. The filter smoothed out high frequency short waves in the horizontal winds but caused only minimal changes in the contravariant vertical velocity.

Domain performance statistics for horizontal wind speed and direction remained almost identical after the filter was applied. However, wind speed and wind direction changed noticeably at some individual grid cells west of the Rocky Mountains.

The domain maximum mass adjustment ratio reduced by approximately 10%, and the standard deviation of the mass adjustment across the domain was reduced by 20-30% in this case.

The domain statistics of ozone concentrations also did not vary significantly. However, large ozone concentration differences were found, especially at some grid cells west of the Rocky Mountains. The filter can lower the predicted minimum ozone concentration as much as 20ppb. Considering that the daily minimum ozone concentrations were overpredicted in the base case, the reductions have the potential of leading to better night time ozone predictions.

## References

- Buyn, D. W., 1999. Dynamically Consistent Formulations in Meteorological and Air Quality Models for Multiscale Atmospheric Studies. Part II: Mass Conservation Issues.
- Byun, D.W., Ching K.S., 1999. Science algorithm of the EPA Models-3 community multiscale air quality (CMAQ) modeling system, USA EPA/600/R-99/030.
- CMAQ v4.6 Operational Guidance Document. available online: [http://www.ie.unc.edu/cempd/products/cmaq/op\\_guidance\\_4.6/html](http://www.ie.unc.edu/cempd/products/cmaq/op_guidance_4.6/html)
- Dudhia, J., 2005. PSU/NCAR Mesoscale Modeling System Tutorial Class Notes and User's Guide: MM5 Modeling System Version.
- Guo, Y, Che Sue. Terrain and Land Use for the Fifth-Generation Penn State/NCAR Mesoscale Modeling System (MM5): Program TERRAIN, NCAR Technical Note, Jan, 1994.
- Odman, M., Russel. A., 2000. Mass conservative coupling of non-hydrostatic meteorological models with air quality models, Air Pollution Modeling and Its Applications. Dordrecht, Kluwer, pp. 651-660.